JOURNAL OF MATERIALS SCIENCE **35** (2000) 2037–2046

New models to explain the compaction and relaxation behaviour of some pharmaceutical excipients submitted to low strain

O. GALLEY, V. LOVERA
Laboratoire de Pharmacie Galénique, Faculté de Pharmacie, 35 chemin des Maraîchers, 31062 Toulouse Cedex France
E-mail: olivier.galley@bms.com

M. VIANA-TRECANT, D. CHULIA
Laboratoire de Pharmacie Galénique, Faculté de Pharmacie, 2 rue du Docteur Marcland, 87025 Limoges Cedex France

J. L. LACOUT
Laboratoire de Physico-chimie des solides, E.N.S.C.T., UPRESA CNRS 5071, 38 Rue des 36 Ponts, 31400 Toulouse France

F. RODRIGUEZ
Laboratoire de Pharmacie Galénique, Faculté de Pharmacie, 35 chemin des Maraîchers, 31062 Toulouse Cedex France

Seven commercially available pharmaceutical excipients used for direct tableting were studied. Flowability, true and tap density, loss on drying, particle size, specific surface area and scanning electron micrographs were used to characterize these powders with low compaction pressures (lower than 10 MPa). The relaxation mode was analysed to describe the behaviour of each product under strain. Three new models are proposed to aid understanding the physical phenomena involved in the compaction phase, and the Peleg model was applied to the relaxation phase. The models were related with the physical properties measured, and illustrate the sliding friction, the viscoelastic behaviour and the aptitude of particles to fragment during compaction, as well as the elastic behaviour during the stress relaxation of powders.

1. Introduction

The main techniques used to analyse the behaviour under strain of direct tableting excipients have been described by several authors, and more recently by Celik [1, 2]. Most study the applied pressure versus punch displacement during compaction [3], obtained with industrial or experimental tablet presses. The machines work at various applied pressures, and compaction speeds and the mode of analysis is varied accordingly. The models usually employed to establish the compaction phenomena involved require high pressures (100 to 400 MPa). The Heckel model for example [4] describes the final part of the compaction phase in the range 50 to 300 MPa which corresponds to the plastic deformation of particles. Studies at a low pressures (lower than 10 MPa) representing the compaction of the particles, are not frequent due to the numerous phenomena involved at the beginning of particle cohesion which are usually difficult to distinguish. Moreover, the standard models (for high pressure) used to study the behaviour of powder under strain cannot be used in this pressure domain. Nevertheless, rheological studies have been performed on food products with a stress relaxation mode at low pressure [5–7], and they have allowed the viscoelastic behaviour of such products to be determined according to the Peleg model [8]. Other authors [9, 10] then investigated the viscoelastic properties of some pharmaceutical excipients by using the stress relaxation mode at low pressure. However, only a few models have been proposed to account for the behaviour of these powders during the compaction phase in this strain range. Our work consists of applying new models to characterize the behaviour of the excipient during compaction and relaxation for applied pressures lower than 10 MPa.

2. Materials and methods

2.1. Materials

The powders used for compression were two microcrystalline celluloses with different particle sizes (Avicel® PH101 and Avicel® PH102, FMC Corp., Philadelphia, PA), two calcium phosphate dihydrates (Encompress®, Edward Mendell, Inc Carmel, NY; Ditab®, Rhone

Poulenc Basic Chemical Co., Shelton, CT), two lactose monohydrates, one obtained by nebulisation (lactose Fast Flo, Foremost Ingredient Group, Baraboo, WI) and the other by granulation (lactose Pharma, French Pharmaceutical Cooperation, Melun, France) and a modified starch (Sta-rx® 1500, Colorcon Inc, West Point, PA). These materials were stored in an atmosphere maintained at 40% humidity, at a temperature of 25°C.

2.2. Equipment for powder compaction

Compaction was performed on a texture analyzer, model TA-XT2 (Rhéo, Champlan, France) instrumented with a strain gauge model 25-1, able to measure forces going up to 245 N, and the data-processing software Texture Expert version 5.16 working with Windows®. The punches used were flat and cylindrical with a diameter of 5 mm. The height of the metal compaction chamber was adjustable.

The compaction speed was 5 mm/s and the maximum applied pressure was 10 MPa. Stress relaxation was observed for 30 seconds. The frequency of data acquisition was 400 Hz. Analyses were performed at constant weight (100 ± 2 mg) and the compaction chamber was gravity-fed.

The reproducibility of measurements was validated, on five samples, by calculating the average, the standard deviation and the coefficient of variation (CV). The threshold of measurement acceptability (coefficient of variation) was fixed at $\pm 10\%$ and was not exceded for any of the parameters studied.

2.3. Powder characteristics

2.3.1. Flow rate

The method used (European Pharmacopeia 3rd Ed.) consisted of measuring the time taken for 100 g of powder to flow through a normalized funnel. It is less than 10 s for a powder that flows easily.

2.3.2. True density

The true density was measured with a gas pycnometer (Acupyc 1330, Micromeritics Instruments Inc., Atlanta, GA), using helium. The sample was vacuum outgased for 2 hours under 15 mm Hg. The measurement was repeated 3 times.

2.3.3. Bulk density and tap density

The apparent bulk density represents the aptitude of a material to become organized without constraint. The method (European Pharmacopeia 3rd Ed.) consisted of pouring 100 g of powder through a 5 mm funnel into a 250 ml graduated cylinder and reading the volume obtained. The tap density was read after 1250 taps (Erweka SVM tapping volumeter, Erweka Gmbh, Hensenstamm, Germany). Three runs were performed for each material.

To compare the behaviour of each excipient, we used the Hausner factor [11] and the Carr index [12]. The Hausner factor is always greater than 1; it increases with the friction between particles and indirectly evaluates the flow rate of powders. The Carr index corresponds to the rearrangement of particles in the powder column and is related to the compressibility in the test conditions.

2.3.4. Particle size analysis

Particle size distribution was measured with laser particle sizer, model LS100Q (Coulter Corporation, Miami, USA) with a Dry Powder Module that permits the analysis of particles suspended in air. The parameters obtained are the median diameter or d_{50} (μm) and the coefficient of variation of the median (%); which is related to the breadth of the particle size distribution.

2.3.5. Specific surface area and porosity

The specific surface area of a powder quantifies the extended solid/gas interface. It was determined by adsorption of nitrogen at the surface of the material (NOVA 1000, Rhéo, Champlan, France). It was calculated by the multi-point B.E.T. method for five relative pressures between 0.05 and 0.3. Porosity was measured during the desorption of nitrogen during the same analysis. The total pore volume and the average pore diameter were obtained by the B.J.H. equation for relative pressures between 0.05 and 0.9. Products were vacuum outgased for 24 hours at 50°C for calcium phosphates, and at 105°C for the other excipients. The measurement was repeated twice for each powder.

2.3.6. Weight loss on drying

Weight loss on drying represents the water adsorbed by the powder. According to Alderborn [13], this water acts as a binder, lubricant and agent of plastic deformation during compaction. Measurements used a thermic infrared weighing machine (Mettler LP16) and followed the method of the European Pharmacopeia 3rd Ed. A weight of approximately 1 g was appropriated and placed at a temperature of 110°C for 20 minutes. Five runs were performed for each material.

2.3.7. Scanning electron microscopy

Scanning electron micrographs of the powder samples, sputtered with a gold/palladium mix: thickness about 50 nm (Ion splutter JFC 1100, JEOL, Croissy sur Seine, France) were taken with a Hitachi S450 apparatus (Elexione, Verrières le Buisson, France). The accelerating voltage is plotted in the photographs. For photographic documentation B/W Ilford FP4 plus film was used.

3. Results and discussion

3.1. Models created for the interpretation of the compaction and relaxation phase

3.1.1. The compaction phase

Compaction can be studied using the equation proposed by Heckel [4] and modified by Schwartz et al. [14]:

$$\ln \frac{1}{1-D} = kP + A - B \exp\, -(\alpha P) \qquad (1)$$

where, D is the relative density or the ratio of apparent density to true density; P is the applied pressure; the constant k is the capacity of the material to deform plastically; α is the coefficient of compressibility due to viscoelastic resistance [14]; A and B are constants.

This model was described by the author for applied pressures (up to 650 MPa) higher than those used in the present work (10 MPa). Nevertheless, this high-pressure model was adjusted to our low-pressure experimental points by:

$$\ln \frac{1}{1-D} = kP + A - (B \exp -(bP) + C \exp -(cP)) \quad (2)$$

The apparent density was measured during the compression. Constants b and c describe the viscoelastic behaviour of the powder during its densification. The lower these constants are, the greater the viscoelastic behaviour of the powder [14]. However, parameter k in this equation had to be redefined for our applied strain.

Fig. 1 shows the compaction phase using the Heckel function. The Heckel plots were separated into three parts or phases A_1, A_2 and A_3 listed in the lactose Pharma plot. These three parts represent, the packing phase (A_1), the viscoelastic behaviour (A_2) and the beginning of the consolidation phase (A_3). An equation can be associated to each part.

$$(A_1) \quad \ln \frac{1}{1-D} = k'P + E \ \text{ for } \ (D_0 < D < D_t) \quad (3)$$

$$(A_2) \quad \ln \frac{1}{1-D} = B \exp -(bP) + C \exp -(cP) \ \text{ for } \ (D_t < D < D_{re}) \quad (4)$$

$$(A_3) \quad \ln \frac{1}{1-D} = kP + A \ \text{ for } \ (D_{re} < D < D_f) \quad (5)$$

D_0 is the relative bulk density of the powder in the compaction chamber, D_t the relative density at the end of particle packing, D_{re} the relative density of the compact after the viscoelastic zone and D_f the final compact density in the compaction chamber. The limits D_t and D_{re} represent the last points from which the coefficient of variation, between the experimental curve and the model is greater than 5%.

In the Heckel plot, the packing phase A_1 represented by a straight line (Equation 3), presents a constant E, and a slope k' we call the coefficient of friction. Indeed, when k' tends to infinity the powder particles organize without opposing resistance, that is to say interparticle and compaction chamber/particle friction is non-existent while punches are moving. The shallower the slope, the more the particles resist organization under strain. When the A_1 phase does not occur, we can consider that the powder rearranges spontaneously in the compaction chamber before compaction.

We determined the relative importance of the packing phase compared to the total phase of compaction, with the percent packing due to packing ($\%D_{pack}$). This constant is obtained with the following equation:

$$\%D_{pack} = \frac{d_t - d_0}{d_f - d_0} \times 100 \quad (6)$$

where d is the apparent density.

Phase A_2 corresponds to the viscoelastic behaviour of the powder. It is represented by an exponential curve (Equation 4), and characterized by two constants b and c. The viscoelastic behaviour of a powder according to Schwartz *et al.* [14] is inversely proportional to the more significant value of the two constants. Thus, we will limit our interpretations to b which is more significant than c.

Phase A_3, with an expression (Equation 5) similar to that of the plastic deformation phase given by the Heckel equation for high pressure, will be discussed in the analysis of results.

3.1.2. The stress relaxation phase

The first step of the stress relaxation study was based on the relative relaxation percentage or $\Delta P / P_{(0)}$ which gives an estimate of the relaxation amplitude for each powder. ΔP is the pressure variation obtained after 30 seconds of relaxation, and $P_{(0)}$ the maximum applied pressure.

For the second step, we used Peleg's model [8] to interpret the behaviour of powders during their relaxation. This model normalizes and linearizes the pressure as a function of time according to the equation:

$$\frac{P_{(0)}t}{P_{(0)} - P_{(t)}} = k_1 + k_2 t \quad (7)$$

$P_{(0)}$ is the maximum initial pressure or applied pressure; $P_{(t)}$ is the pressure recorded after time t; k_1 is a constant related to the initial speed decrease of the pressure; k_2 has no dimension and represents the elastic behaviour of the excipient. A purely viscous substance relaxes totally ($k_2 = 1$), while an ideal elastic substance does not relax at all ($k_2 \to \infty$).

According to the author, this model is suitable for use when the experimental relaxation curve (applied pressure versus time) is represented by an exponential equation with 3 or 4 terms. These equations and their correlation coefficients for each excipient are reported in Table I, and show that all the powders tested verify this rule. Nevertheless, Peleg's model was established for an open system with food products. In our case, the analyses were made on powder in a closed system limited by the compaction chamber. It can, however, be adapted to our device if we consider that the axial pressure applied and the radial forces due to the sides of the compaction chamber are measured. It gives an estimation of the viscoelastic behaviour of our excipients during stress relaxation.

3.2. Rheological and physical properties

The direct tableting excipients were first characterized by weight loss on drying, the bulk, true and relative

TABLE I Exponential decay equations of relaxation curves for each excipient, and the coefficient of correlation *r*

Excipient	Exponential decay equation of $P_{(t)}$ (MPa) versus t(s)	*r*
Avicel® PH101	$P_{(t)} = 1.112\exp(-15.63\,t) + 0.663\exp(-0.92\,t) + 8.234\exp(-1.4\,10^{-3}\,t)$	0.9973
Avicel® PH102	$P_{(t)} = 1.194\exp(-15.83\,t) + 0.697\exp(-0.95\,t) + 8.201\exp(-1.4\,10^{-3}\,t)$	0.9980
Encompress®	$P_{(t)} = 0.247\exp(-12.16\,t) + 0.276\exp(-0.76\,t) + 9.789\exp(-3\,10^{-4}\,t)$	0.9964
Ditab®	$P_{(t)} = 0.272\exp(-16.55\,t) + 0.296\exp(-0.92\,t) + 9.777\exp(-4\,10^{-4}\,t)$	0.9957
Lactose Pharma	$P_{(t)} = 0.578\exp(-14.16\,t) + 0.354\exp(-0.95\,t) + 9.549\exp(-4\,10^{-4}\,t)$	0.9981
Lactose Fast Flo	$P_{(t)} = 1.387\exp(-12.05\,t) + 1.097\exp(-0.69\,t) + 7.751\exp(-3.1\,10^{-3}\,t)$	0.9985
Sta-rx 1500	$P_{(t)} = 0.963\exp(-11.43\,t) + 0.654\exp(-0.76\,t) + 8.583\exp(-1.3\,10^{-3}\,t)$	0.9987

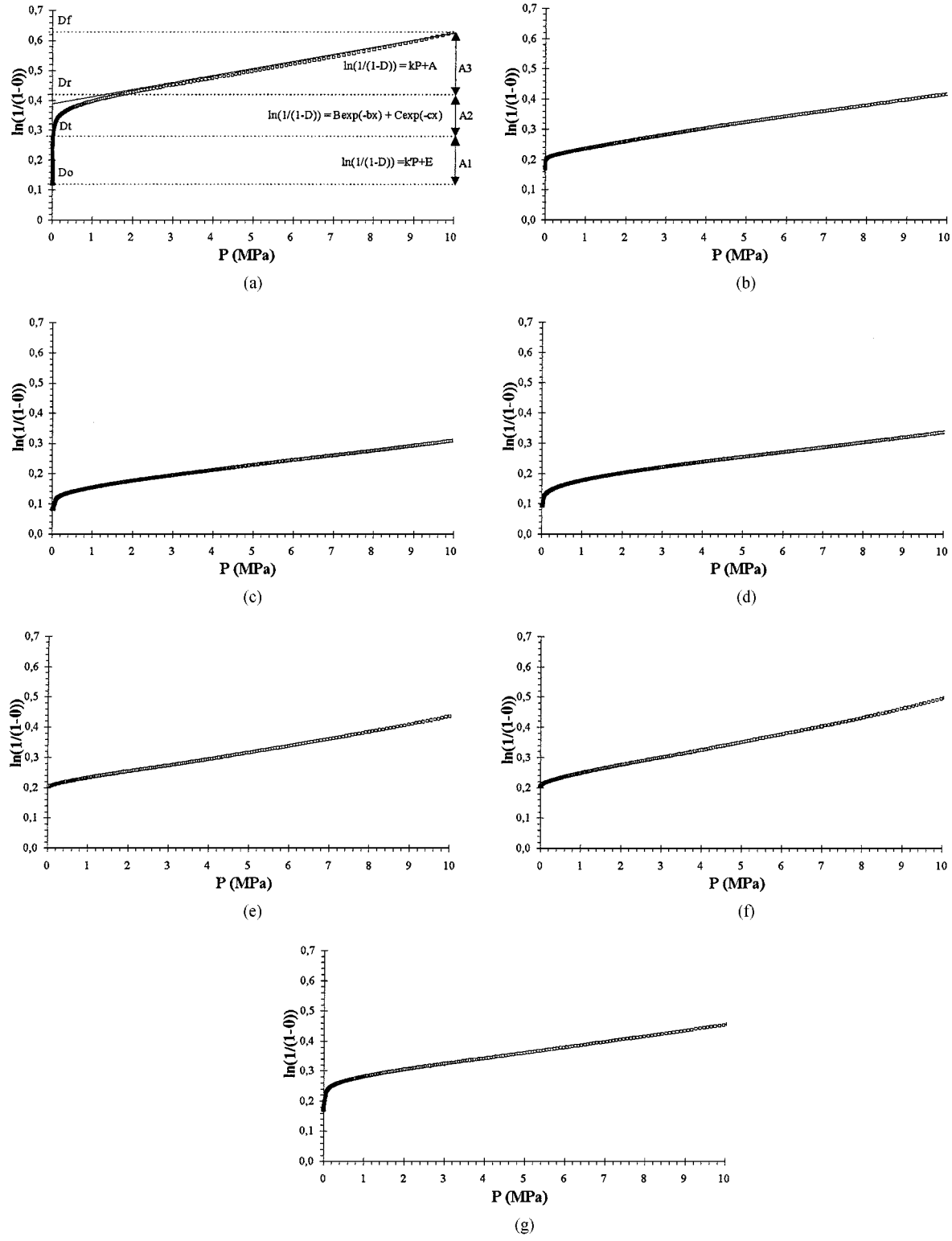

Figure 1 Heckel plot at 10 MPa pressure for the following excipients: (a) Lactose Pharma; (b) Lactose Fast Flo; (c) Avicel® PH101; (d) Avicel® PH102; (e) Encompress®; (f) Ditab®; (g) Sta-rx® 1500.

TABLE II Powder characteristics of the excipients

Excipient	Loss on drying (%)	Bulk density (g/cm^3)	True density (g/cm^3)	Relative density	Hausner factor	Carr index (%)	Flow rate (s)
Avicel® PH101	6.25 ±0.56	0.29 ±0.010	1.54 ±0.04	0.188	1.60	37.65	∞
Avicel® PH102	6.01 ±0.08	0.32 ±0.012	1.59 ±0.06	0.201	1.65	39.35	7.0 ±0.22
Encompress®	2.51 ±0.53	0.89 ±0.011	2.29 ±0.06	0.388	1.09	8.04	3.0 ±0.15
Ditab®	1.09 ±0.20	0.86 ±0.009	2.31 ±0.05	0.372	1.12	10.34	3.5 ±0.26
Lactose Pharma	0.98 ±0.04	0.53 ±0.013	1.51 ±0.09	0.351	1.17	14.21	∞
Lactose Fast Flo	1.06 ±0.04	0.52 ±0.008	1.52 ±0.01	0.342	1.20	16.67	5.0 ±0.46
Sta-rx® 1500	10.55 ±0.49	0.58 ±0.005	1.56 ±0.07	0.372	1.18	15.12	∞

densities, the Hausner factor, the Carr index and the flow rate. These parameters are reported for each excipient in Table II.

Weight loss on drying shows little adsorbed water for the calcium phosphates and the lactoses (less than 2.5%), while for the celluloses and especially the modified starch, the amount of adsorbed water was higher (over 6%). Starch is known to be particularly hygroscopic.

The relative density, represented by the ratio to the bulk density to the true density, illustrates that celluloses have the lowest values (less than 0.2) and therefore the least organized particles compared to all the other excipients (relative densities between 0.342 and 0.388). The highest value was measured for Encompress®.

The Hausner factor for celluloses (≈1.6) indicates high inter-particle friction which prevents the powder from flowing freely.

In order to compare the excipient behaviour more precisely, we used the classification given by Carr [12]. According to this classification, our results indicate the flow capacity as being excellent for calcium phosphates, good for lactoses and starch, and poor for celluloses.

Finally, the flow rate measurement showed that Avicel® PH101, lactose Pharma and Sta-rx® 1500 flow badly (flow rate $\rightarrow \infty$) in comparison to the other excipients ($t \leq 7.0$ s). For starch, we considered this was due to the large quantity of adsorbed water. Complementary analyses were then performed to characterize each excipient more fully.

The contact area and the particle size play an essential role in flow and in the organization of the powder bed, as well as in the cohesion of the final product. For each excipient, we therefore measured the particle size, the specific surface area and the porosity of the particles. The results are reported in Table III.

The median particle size gave the following rank order:

TABLE III Particle characteristics of the excipients

Excipient	d_{50} (μm)	CV (%)	Specific surface area (m^2/g)	V_p 10^{-3} (cm^3/g)	r_p (Å)
Avicel® PH101	71.3 ±2.7	59.3 ±1.3	1.83 ±0.10	2.71 ±0.03	29.51 ±0.56
Avicel® PH102	146.8 ±5.6	58.0 ±2.6	1.42 ±0.16	2.18 ±0.05	30.60 ±0.49
Encompress®	180.8 ±3.1	39.2 ±3.3	4.53 ±0.36	9.30 ±0.06	41.05 ±1.35
Ditab®	159.5 ±4.8	39.7 ±2.7	3.27 ±0.25	5.92 ±0.18	36.19 ±1.67
Lactose Pharma	67.0 ±2.4	92.4 ±2.0	2.60 ±0.28	3.18 ±0.08	24.47 ±0.68
Lactose Fast Flo	108.3 ±6.4	42.7 ±1.0	2.94 ±0.18	4.13 ±0.36	28.16 ±0.92
Sta-rx® 1500	93.1 ±1.9	56.5 ±3.7	1.04 ±0.09	0.84 ±0.02	16.22 ±0.26

The median variation coefficient shows little displaying of all powders (less than 60%) except for lactose Pharma (92.4%). These results and those given above show that the particle size two times larger for Avicel® PH102 than for Avicel® PH101 tends to improve flowability. Moreover, the low value of the median of lactose Pharma (67.0 μm) and breadth of its distribution, due to a large proportion of fine particles, are factors unfavourable for flow.

For a large increase in the particle size, the specific surface area of microcrystalline celluloses only decreases slightly, without modification of the average pore radius. The flow of these celluloses seems to be influenced more by the particle size than by the specific surface area and the porosity. The calcium phosphates had the greatest specific surface areas (>3.2 m^2/g), as well as particle pore volumes and radii. We can note that for Encompress® the pore volume is about twice as high as for Ditab®. This could be due to the average pore radius which is a little greater for Encompress®. Lactose

Emcompress® > Ditab® > Avicel® PH102 > lactose Fast Flo > Sta-rx®1500 > Avicel® PH101 > lactose Pharma

TABLE IV Compaction parameters for each excipient by model

Phase	A_1				A_2			A_3	
Excipient	d_0 (g/cm^3)	$\%D_{pack}$ (%)	k' (MPa^{-1})	r	b (MPa^{-1})	c (MPa^{-1})	r	$k\ 10^{-3}$ (MPa^{-1})	r
Avicel® PH101	0.263 ±0.019	19.8	0.94	0.9904	1.09 ±0.01	9.68 ±0.34	0.9999	37.4 ±0.26	0.9999
Avicel® PH102	0.303 ±0.007	16.3	2.09	0.9245	1.11 ±0.01	9.78 ±0.20	0.9998	37.1 ±0.35	0.9999
Encompress®	0.878 ±0.024	—	—	—	—	—	—	51.4 ±0.21	0.9990
Ditab®	0.883 ±0.017	—	—	—	—	—	—	61.6 ±1.08	0.9990
Lactose Pharma	0.375 ±0.046	38.9	∞	—	2.86 ±0.18	29.02 ±1.93	0.9950	55.9 ±0.17	0.9995
Lactose Fast Flo	0.501 ±0.008	11.0	6.70	0.4421	0.64 ±0.01	32.44 ±1.55	0.9969	43.4 ±0.39	0.9997
Sta-rx® 1500	0.504 ±0.025	19.3	2.15	0.9573	1.83 ±0.07	21.68 ±1.19	0.9965	42.9 ±0.86	0.9999

Fast Flo develops a specific surface area slightly higher than that of lactose Pharma. By referring to the total pore volume and radius, lactose Fast Flo particles are seen to be more porous than those of the lactose Pharma. Finally, the negative influence of adsorbed water in Sta-rx® 1500 concerning flowability seems to be confirmed, since neither its average particle size, nor its low specific surface area (1.04 m^2/g) can be considered as unfavourable factors for the flow of the powder.

3.3. Powder compaction

Table IV lists the initial apparent density d_0, the percentage of compaction $\%D_{pack}$, slopes k and k', constants b and c, and the correlation coefficient of each model, for all excipients. Initial apparent densities (d_0) measured in the compaction chamber are equivalent to bulk densities, for all excipients except lactose Pharma (bulk density of 0.53 g/cm^3 for a d_0 equal to 0.375 g/cm^3) and Sta-rx® 1500 (bulk density of 0.58 g/cm^3 for a d_0 equal to 0.504 g/cm^3). For these two excipients, this can be ascribed to the problem of flow already observed when determining the flow rate through a funnel. In addition, the results show that the filling of the compaction chamber by gravity does not cause preliminary compaction of the powder.

The data for densification due to packing ($\%D_{pack}$), show that calcium phosphates have no packing phase. This confirms previous conclusions about the good flow properties and the homogeneous and rapid organization of particles in this type of excipient. The same observation was made for lactose Fast Flo; its high flow limiting the importance of this phase ($\%D_{pack} = 11\%$). Lactose Pharma presents a very strong compaction phase (up to 39%), that we attribute to its small particle size and broad size distribution leading to poor flow.

Fig. 1 represents the excipient compaction. Each phase will be commented on in the order in which it occurs.

3.3.1. The packing phase (A_1)

In the very low pressure range, the lactose Pharma graph shows, according to our model (Equation 3), a k' slope that tends to infinity. We attribute this absence of sliding friction under pressure to the large interparticle voids present in the column of powder, causing poor flow due to small particle size. For lactose Fast Flo, there was a weak coefficient of regression despite a homogeneous distribution of experimental points around the straight line calculated with our model. The model is not therefore representative of the actual excipient. The steep slope for lactose Fast Flo ($k' = 6.70$ MPa^{-1}) can be interpreted by a low sliding friction of particles during their forced reorganization. The celluloses and the starch showed a high resistance to particle organization under strain ($k' \leq 2.09$ MPa^{-1}). For celluloses, this resistance increases as the particle size decreases. For a given volume of powder, this can be easily explained taking into account the increase in the number of contacts between particles when the particles size decreases. Cross analysis of the initial apparent densities (d_0), the percentage of compaction and the slope k' shows the same behaviour as for the Carr index, the Hausner factor and the flow rate test for each product.

3.3.2. The viscoelastic behaviour (phase A_2)

The constant b calculated from our model (Equation 4) shows that lactose Fast Flo presents the highest viscoelastic resistance ($b < 0.7$ MPa^{-1}). The viscoelastic resistance was lower for microcrystalline celluloses and does not depend on the particle size of the product. For lactose Pharma and Sta-rx® 1500, the viscoelastic resistance is the lowest, with a value of the constant b superior to 2.5 MPa^{-1} for lactose Pharma. The compaction plots of calcium phosphates show a very weak involvement of phase A_2 that does not allow us to interpret the results. Comparison of the results obtained during phases A_1 and A_2, reveals the role of the packing phase in the viscoelastic resistance of the powder. Indeed, the higher the percentage of compaction ($\%D_{pack}$ increases), the less the powder exerts viscoelastic resistance during its densification (b increases). Nevertheless, for an equivalent value of k' for Avicel® PH102 and Sta-rx® 1500 ($k' \approx 2.10$ MPa^{-1}), we observe values of b equal to 1.11 and 1.83 MPa^{-1} respectively, showing

that sliding friction is not the only parameter involved in this phase.

3.3.3. The consolidation phase (phase A_3)

The phase of consolidation or agglomeration represented by a straight line of slope k (Equation 5, Table IV) enables excipients to be ranked in decreasing order of the slope:

Ditab® > lactose Pharma > Emcompress® > lactose Fast Flo ≈ Sta-rx®1500 > Avicel® PH102 ≈ Avicel® PH101

According to Nyström *et al.* [15], the study of the densification of pharmaceutical excipients shows that at high strain calcium phosphate dihydrates and lactoses are fragmenting materials, and starches and microcrystalline celluloses are plastically deforming materials. In addition, in our range of pressures (under 10 MPa) the slope k does not represent the capacity of a powder to deform plastically, as Heckel describes it [4], because this behaviour is mainly observed for higher pressures

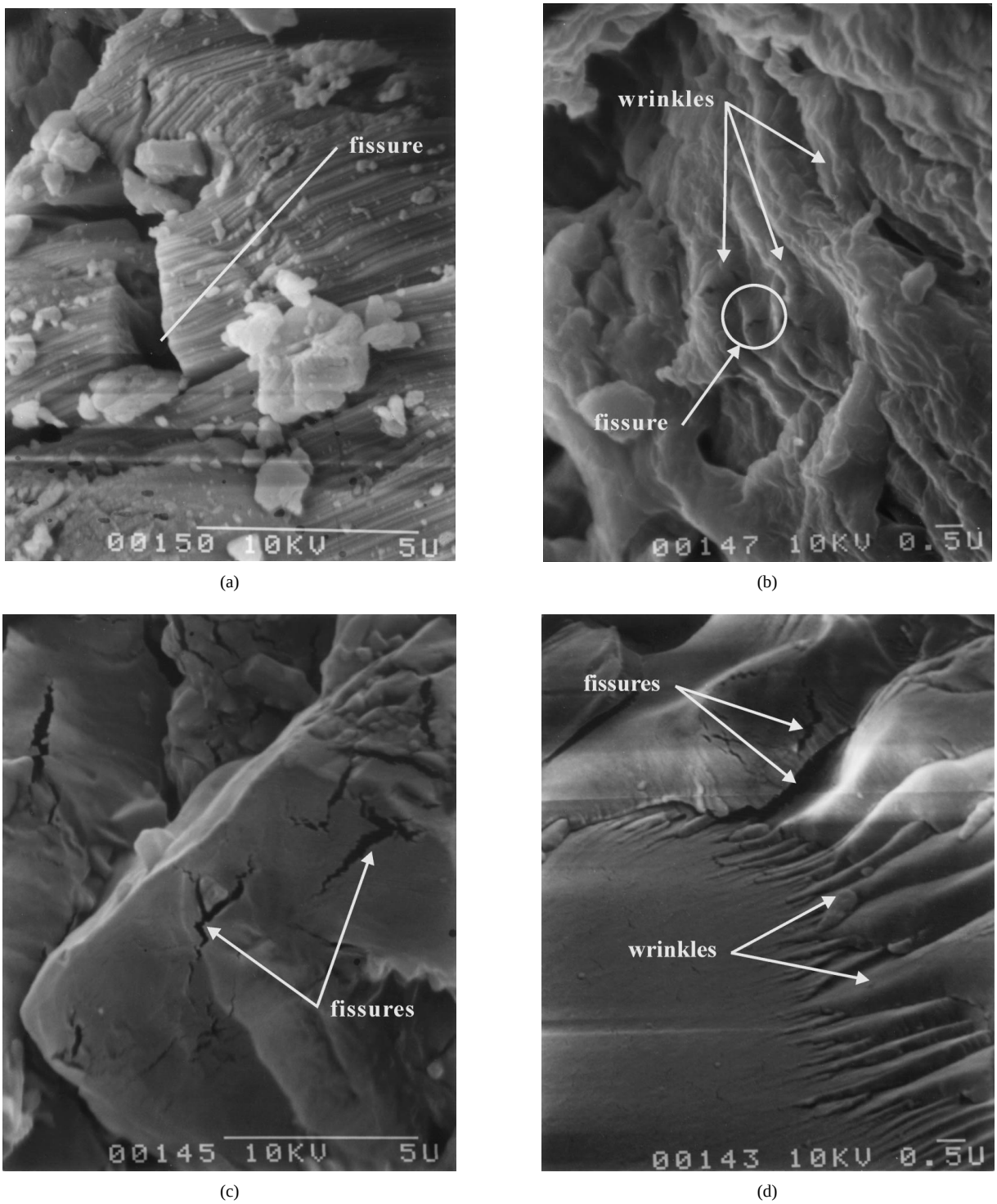

Figure 2 Surface of an excipient particle contained in a tablet compacted at a pressure of 6 MPa: (a) Ditab® (magnification ×9000); (b) Avicel® PH101 (magnification ×10000); (c) Fast Flo (magnification ×7900); (d) Sta-rx® 1500 (magnification ×10000).

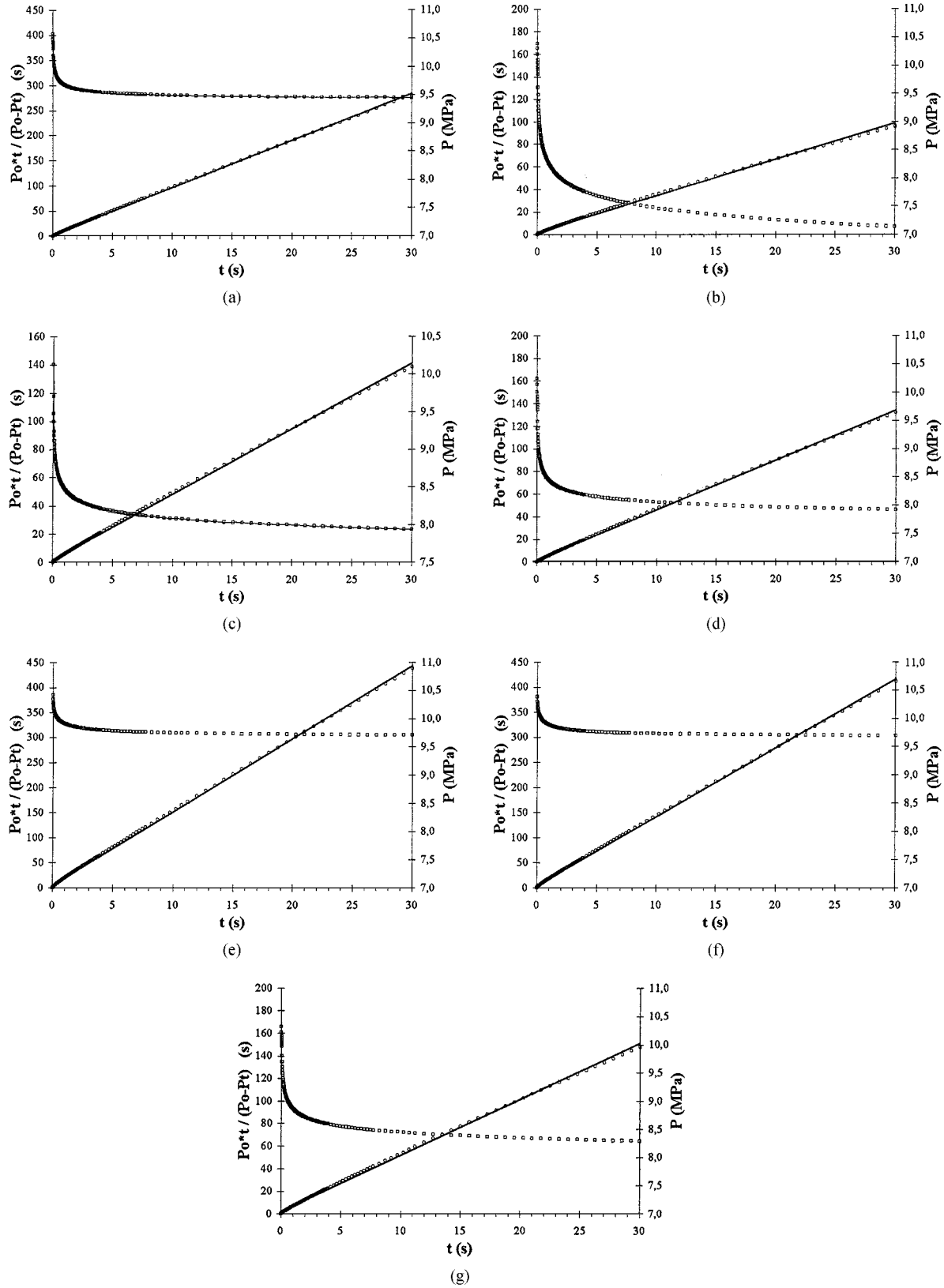

Figure 3 Exponential and linearized stress relaxation curves plotted with Peleg's model. (□ Stress relaxation plot, ● Peleg's experimental points, —Peleg's straight line plot): (a) Lactose Pharma; (b) Lactose Fast Flo; (c) Avicel® PH101; (d) Avicel® PH102; (e) Encompress®; (f) Ditab®; (g) Sta-rx® 1500.

(over 50 MPa). The works of Gonthier [16], based on the use of the Heckel plot at low pressures (between 0 and about 50 MPa), show that the curvature observed at low pressure accounts for the rearrangement and/or the fragmentation of the particles. In our work, the pressure range used for the calculation of k was lower than that of Gonthier, but the maximum applied pressure was sufficient to cause rupture of the particles. We can therefore suggest that the constant k describes the fragmentary behaviour of the excipients. To verify this hypothesis, we studied the particle structure once compacted by means of a scanning electron microscope (Fig. 2). The study was performed on four of the seven excipients taking into account their classification according

to their k values. They were Ditab® and Avicel® PH101 which were at the extremes of this classification, and lactose Fast Flo and Sta-rx® 1500 which have a different compaction mode under strain for an identical value of k. The tablets were obtained by applying a pressure of 6 MPa which corresponds to the middle of the straight line of our model for phase A_2. Ditab® shows large fissures on the surface of the grains as well as many smaller particles generated by fragmentation. For Avicel® PH101, wrinkles appeared on the particle surface due to plastic deformation of the structure and very small fissures, not creating new particles, showed the slight fragmentary behavior of this product. For lactose Fast Flo, very large fissures occurred without the creation of new particles. This observation indicates that the structure of the particle was weakened although its integrity was not affected. Finally for Sta-rx® 1500, many wrinkles are clearly visible as well as a few fissures that do not seem to form new particles. These results confirm our hypothesis for these products. Indeed constant k is related to the tendency of a powder to fragment, indicating the friability of the particles.

The higher the value of k, the more fragmentary behaviour the powders present during densification. Indeed, Ditab® ($k = 61.6 \times 10^{-3}$ MPa^{-1}) is more friable than the Encompress® ($k = 51.4 \times 10^{-3}$ MPa^{-1}), in agreement with the works of Muñoz Ruiz [17] performed at higher pressures. Lactose Pharma is more friable under pressure than lactose Fast Flo and Sta-rx® 1500. Finally, celluloses have the lowest value of k ($k < 38 \times 10^{-3}$ MPa^{-1}) which is always independent of the particle size.

3.4. The relaxation phase

Fig. 3 plots stress relaxation versus time for each excipient as well as the straight line calculated from Peleg's model. The relative relaxation percentage $\Delta P/P_{(0)}$, the constants k_1 and k_2 (Equation 7) for each excipient, and the coefficients of correlation are reported in Table V.

The percentage relaxation of lactose Fast Flo is high (31.05%). The celluloses and the starch present an equal but lower relaxation. Finally, the calcium phosphates and lactose Pharma show the lowest stress relaxation ($\Delta P/P_{(0)} \leq 10\%$), the value for lactose Pharma being slightly higher than for the calcium phosphates.

Peleg's model shows that calcium phosphates have the highest values of k_2 (>13.6) which indicate high elasticity of the tablet under pressure. Moreover, the high value of k_1 (≈ 5 s) indicates a slow relaxation speed. With lactose Pharma, the high elasticity leads to a faster relaxation speed. For celluloses, the increase of particle size had no significant effect on the elastic behaviour or the relaxation speed. Rheologically, the celluloses and starch are less elastic or more "viscous" than the other excipients. This "viscous" behaviour was greatest for lactose Fast Flo ($k_2 = 3.22$), for a rapid relaxation speed. Therefore, according to the elastic response indicated by the value of k_2, we obtain the following classification:

TABLE V Relaxation parameters obtained by Peleg's model for each excipient

Excipient	$\Delta P/P_{(0)}$ (%)	k_1 (s)	k_2	r
Avicel® PH101	22.12	1.68	4.64	0.9997
	±0.33	±0.08	±0.009	
Avicel® PH102	22.92	1.39	4.41	0.9997
	±0.23	±0.06	±0.008	
Encompress®	7.05	5.67	14.57	0.9997
	±0.28	±0.03	±0.025	
Ditab®	6.72	4.63	13.69	0.9998
	±0.18	±0.05	±0.021	
Lactose Pharma	10.02	2.43	9.34	0.9999
	±1.03	±0.09	±0.011	
Lactose Fast Flo	31.05	1.79	3.22	0.9991
	±1.26	±0.15	±0.010	
Sta-rx® 1500	20.52	1.97	4.96	0.9996
	±1.38	±0.11	±0.011	

This rank order is in agreement with results obtained by calculating the relative relaxation percentage, and confirms that Peleg's model is applicable to our method of analysis.

From our interpretation of slope k in our model, we can conclude that the more the powder shows fragmentary behaviour during compaction, the greater the elastic response during stress relaxation.

4. Conclusion

In this work, we studied the behaviour of some powdered pharmaceutical excipients during low pressure compaction, and stress relaxation. We observed that the flow and the particle size of such powders accounts for the degree of packing during their densification. Moreover, in the materials investigated, powders which fragment under pressure show high elasticity during stress relaxation. The models that we used to describe the phenomena involved in the densification of powders showed the important role of particle sliding friction during the packing phase, the viscoelastic behaviour during the intermediate phase, and the aptitude of particles to fragment during the final compaction. Finally, Peleg's model applied to the relaxation phase revealed the elastic response of tablet formed at low pressure.

Acknowledgement

We greatly indebted to the UPSA company for financing this study and supplying the materials.

References

1. M. CELIK, *Drug Dev. Ind. Pharm.* **18** (1992) 767.
2. *Idem., ibid.* **22** (1996) 1.
3. J. C. GUYOT, A. DELACOURTE, P. BLEUSE and P. LETERME, *Sci. Tech. Pharm.* **263** (1982) 427.
4. R. W. HECKEL, *Trans. Metall. Soc. AIME.* **221** (1961) 671.
5. M. PELEG and M. D. NORMAND, *Rheol. Acta.* **22** (1983) 108.
6. Y. NOËL and C. ACHILLEOS, *Cahier de Rhéologie.* **15**(4) (1997) 568.

Encompress® > Ditab® > lactose Pharma ≫ Sta-rx® 1500 > Avicel® PH101 > Avicel® PH102 > lactose Fast Flo

7. P. SABRE, Y. BOURTEL, F. BOUVIER and M. SERPELLONI, *ibid.* **15**(4) (1997) 574.
8. M. PELEG, *J. Food Sci.* **44** (1979) 277.
9. P. CARMONA, P. MICHAUD, J. F. CORDOLIANI, D. CHULIA and F. RODRIGUEZ, *Cahier de Rhéologie.* **13**(4) (1996) 807.
10. C. LANOS and A. VUEZ, *ibid.* **15**(4) (1997) 21.
11. H. H. HAUSNER, *Int. J. Powder Metall.* **3** (1967) 7.
12. R. L. CARR, *Chem. Eng.* **18** (1965) 163.
13. G. ALDERBORN and C. AHLNECK, *Int. J. Pharm.* **73** (1991) 249.
14. J. SCHWARTZ, N. H. NGUYEN and R. L. SCHNAARE, *Drug Dev. Ind. Pharm.* **20**(20) (1994) 3105.
15. C. NYSTRÖM, G. ALDERBORN, M. DUBERG and P. G. KAREHILL, *ibid.* **19** (1993) 2143.
16. Y. GONTHIER, Doctoral thesis, Pharmaceutical Sciences, Grenoble **I** 1984.
17. A. MUÑOZ RUIZ, T. PAYÀN VILLARD, N. MUÑOZ MUÑOZ, M. C. MONEDERO PERALES and M. R. JIMÉNEZ-CASTELLANOS, *Int. J. Pharm.* **110** (1994) 37.

Received 18 June 1998
and accepted 14 January 1999